

Phase-ordering dynamics of nematic liquid crystals

R. E. Blundell and A. J. Bray

Department of Theoretical Physics, The University, Manchester M13 9PL, England

(Received 30 June 1992)

We study phase ordering in nematic liquid crystals using cell-dynamics simulations for $d=2, n=2$ and $d=3, n=3$. The tail in the structure function decays as $k^{-\chi}$, with $\chi=4.0 \pm 0.1$ for $d=2$ and $\chi=5.3 \pm 0.1$ for $d=3$. We compare these values to results of Bray and Puri [Phys. Rev. Lett. **67**, 2670 (1991)] for a vector order parameter and to experimental measurements. For the $d=3$ system the characteristic length scale in the system varies as $L(t) \sim t^\phi$, with $\phi=0.44 \pm 0.01$.

PACS number(s): 61.30.-v, 64.60.Cn, 64.60.My

The phase-ordering dynamics of systems with a continuous as opposed to a discrete symmetry has been a subject of theoretical interest for some time [1-8]. Attention has focused on the $O(n)$ model and in particular its continuum description by the time-dependent Ginzburg Landau equation [7,8]. A number of analytic predictions have been made, both for the dynamics of individual defects [9] and for the form of the correlation function and structure factor [7,8]. The most striking of these is that the structure function should exhibit a power-law tail of the form $S(k,t) \sim l(t)^{-n} k^{-(d+n)}$ for $kl(t) \gg 1$, where $l(t)$ is the characteristic scale of the order at time t . This result generalizes the familiar "Porod's law" [10] for scalar systems, and is consistent with results from numerical simulations [2,3,11].

More recently it has been recognized [4,5] that nematic liquid crystals (NLC's) provide an experimentally accessible system with which to compare these predictions. Like the $O(n)$ model, they have a continuous symmetry, but one that belongs to a different homotopy class. The rod-like molecules that form a liquid crystal have an inversion symmetry that the vector spins in the $O(n)$ model lack. The vacuum manifold for the bulk nematic is therefore the projective two-sphere $\mathcal{S}_2/\mathcal{Z}_2$ instead of the simple two-sphere \mathcal{S}_2 . One consequence of this additional symmetry is to create topological defects not present in the $O(n)$ model, in particular the $\pm \frac{1}{2}$ string [12]. Considerable work has been devoted to understanding the dynamics of these defects, both in isolation [13] and in the bulk system [4].

The direct comparison of theoretical results derived for the $O(n)$ model and experimental data from NLC's is difficult. The inversion symmetry of the "spins" in a liquid crystal may lead to modifications of the phase ordering. Furthermore, the local energy density is not as simple as that of the $O(n)$ model. This too may affect the behavior. We return to this point later.

The aim of the simulations was to investigate the effect of the modified symmetry in NLC's on the ordering dynamics and, in particular, to compare the form of the structure factor to a recent result for the $O(n)$ model by Bray and Puri [7]. We also make comparisons both with experimental results for liquid crystals [14] and with previous simulations [2,3,11] and analytic work [7,8] for systems with $O(n)$ symmetry.

The model we have used for the simulations is defined by

$$H = - \sum_{\langle i,j \rangle} (\phi_i \cdot \phi_j)^2, \quad (1)$$

where ϕ_i is the usual $O(n)$ vector spin. This model might be termed a "spin nematic." There is an effective field $h_i = \sum_j (\phi_i \cdot \phi_j) \phi_j$ at site i , and we consider the equation of motion

$$\frac{\partial \phi_i}{\partial t} = \sum_j (\phi_i \cdot \phi_j) \phi_j - \sum_j (\phi_i \cdot \phi_j)^2 \phi_i, \quad (2)$$

which preserves the length of the spins. This equation is invariant under a local transformation $\phi_k \rightarrow -\phi_k$ at any site k and so incorporates the effect of a spin inversion symmetry into the $O(n)$ model. It is also invariant under internal and spatial rotations separately, which is not in general the case in a liquid crystal. The true equations of motion for a liquid crystal are more complicated; the local energy density is often written as [15]

$$\mathcal{E} = \frac{1}{2} \{ K_1 (\nabla \cdot \phi)^2 + K_2 (\phi \cdot \nabla \times \phi)^2 + K_3 [\phi \times (\nabla \times \phi)]^2 + K_4 \nabla \cdot [(\phi \cdot \nabla) \phi - \phi (\nabla \cdot \phi)] \}, \quad (3)$$

where the K_i are constants characteristic of a particular liquid crystal. This expression is now only invariant under rigid rotations of the external and internal spaces together but if the K_i are all equal then, ignoring the last term which is a surface term, the energy density can be written in the more compact form

$$\mathcal{E} = \frac{K}{2} (\partial_a \phi^b)^2, \quad (4)$$

which now is invariant under spatial and internal rotations independently. This is the frequently used "one-constant" approximation [15]. As our model has the same symmetry properties we expect it to produce dynamics equivalent to those of a liquid crystal with equal K_i . Using the director field, rather than the full traceless, symmetric, tensor order parameter also leads to a simpler and faster simulation code, while losing none of the essential physics.

We have used a cell-dynamics scheme [16] to simulate this model. We treat the ϕ as "soft" spins and use the

discrete-time updating relation

$$\phi_{n+1}(i) = D \left[\frac{1}{z} \sum_j [\hat{\phi}_n(i) \cdot \hat{\phi}_n(j)] \phi_n(j) - \phi_n(i) \right] + E \hat{\phi}_n(i) \tanh(|\phi_n(i)|), \quad (5)$$

where z is the number of nearest neighbors of a site. It is necessary to make two of the vectors in the first term unit vectors otherwise the iteration process becomes unstable. The arrangement above appears to be the best choice: taking both the $\phi(j)$ as unit vectors tends to lead to a freezing of the spins in some metastable configuration. D and E are adjustable parameters, usually taken to be $D=0.5$ and $E=1.3$ for scalar fields [16]. We used these values for the $d=3$ system. For the $d=2$ system however, we found that to avoid freezing of the spins $D=1.0$ and $E=1.1$ were a better choice. This corresponds to a larger vortex core size, which allows the defects more freedom to move. To simulate a quench from the isotropic to the nematic phase we initially set all the $\phi(i)$ to have random orientations and unit length. We investigated the effect of starting with vectors of random length as well as random orientation, but this made no difference to the results.

We ran simulations of a two-component vector in two dimensions and a three-component vector in three dimensions corresponding to a thin film and a bulk nematic liquid crystal, respectively. In both cases we calculated the correlation function

$$C(r) = [1/(d-1)] \langle d(\hat{\phi}(0) \cdot \hat{\phi}(r))^2 - 1 \rangle$$

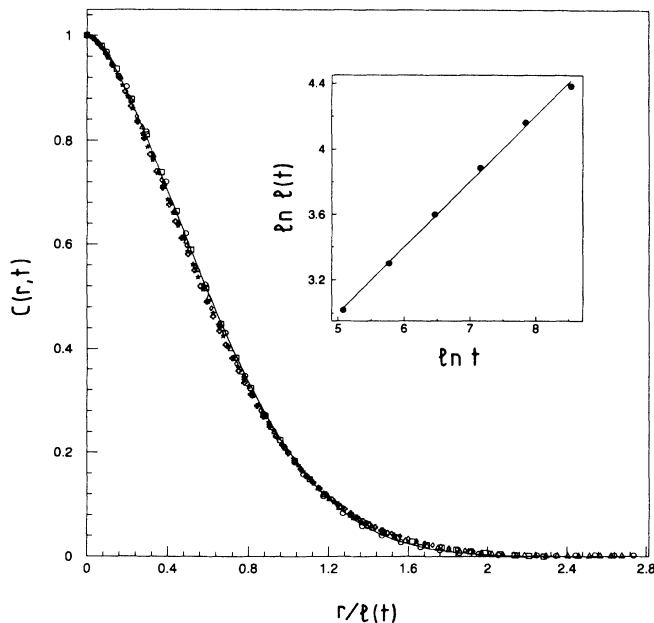


FIG. 1. Scaling plot of the correlation function $C(r,t)$ against $r/l(t)$ for a 2D nematic liquid crystal. The data were taken from a 500^2 lattice, averaged over 20 initial conditions. The symbols correspond to times 160 (\circ), 320 (\square), 640 (\triangle), 1280 (\diamond), 2560 (\oplus), and 5120 ($*$) cell dynamics steps. The length scale $l(t)$ is defined by $C(l(t),t)=0.2$. The solid curve is the Bray-Puri function [7] for $n=2$. The inset shows a plot of $\ln l(t)$ vs $\ln t$. The straight line has a slope 0.4.

and the structure function $S(k) = \sum_r C(r) \exp(-ik \cdot r)$, without spherically averaging (i.e., k was taken along lattice axes only). The definition of C ensures that the local inversion symmetry of the spins is respected; making the spins unit vectors “hardens” them, effectively reducing the vortex core size to zero. We expect this to improve the scaling for large $kl(t)$ at early times [17]. Assuming dynamic scaling holds for the NLC, the correlation function and structure factor have the scaling forms

$$C(r,t) = f(r/l(t)), \quad (6)$$

$$S(k,t) = l(t)^d g(kl(t)). \quad (7)$$

For the $d=2$ simulation, we used $l(t)$ defined by $C(l(t),t)=0.2$ to scale both $C(r,t)$ and $S(k,t)$ [18]. The results are shown in Figs. 1 and 2. We used a lattice of 500^2 spins with periodic boundary conditions, averaging over 20 sets of initial conditions and running for up to 5120 lattice updates. For the time scales investigated the data are not consistent with a simple power-law dependence $l(t) \sim t^\phi$ (see inset, Fig. 1). We have also tried to fit $l(t)$ to a function of the form $\ln(t)/t^\phi$, but again without success. However, the quality of the scaling collapse for the $C(r,t)$ data is quite acceptable.

Figures 3 and 4 show the results for the $d=3, n=3$ system. Here we were able to scale the data using $l(t) \sim t^{0.44}$ over time scales between 40 and 1200 updates (inset, Fig. 3). Comparison of data for $L=64$ and $L=90$ shows no evidence of any finite-size effects.

Bray and Puri (BP) [7] have recently shown that, for systems with an n -component vector order parameter, the structure function decays for large kl as $S(k) \sim l^{-n} k^{-\chi}$, with $\chi = d + n$. A simple derivation of this result has recently been given by Bray [19], based on the observation

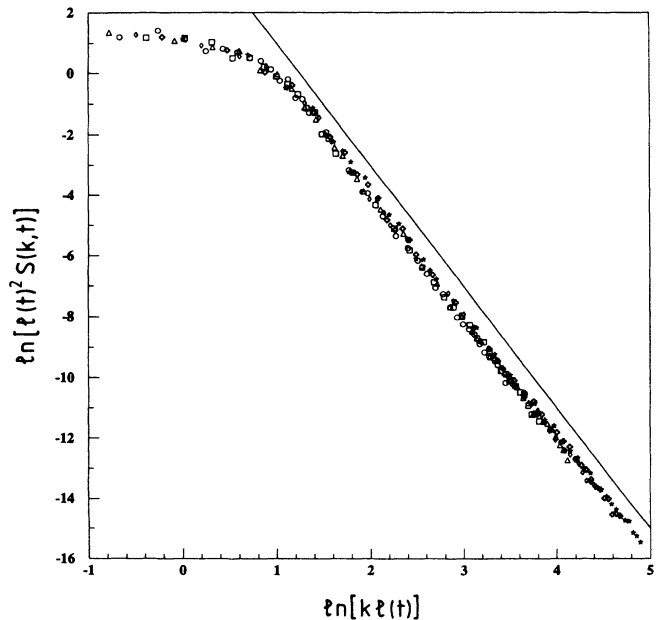


FIG. 2. Log-log scaling plot for the structure function of the 2D nematic liquid crystal. Only k values up to $\frac{1}{2}$ of the zone boundary are included. The symbols have the same meanings as in Fig. 1. The straight line has a slope -4 .

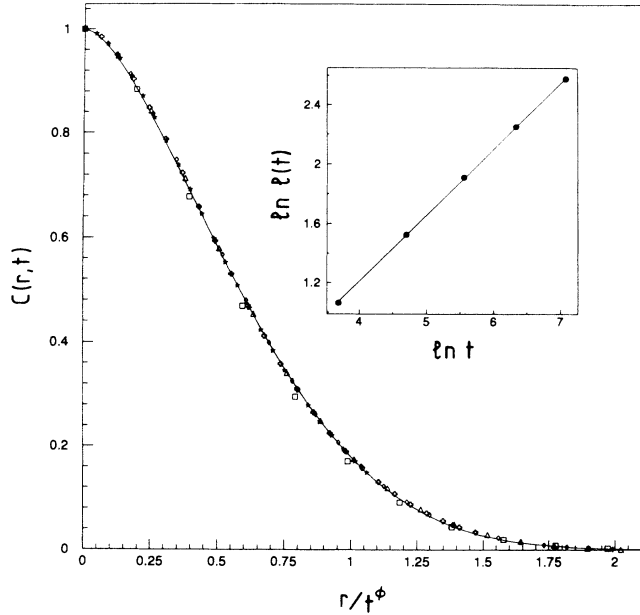


FIG. 3. Scaling plot of the correlation function $C(r,t)$ against r/t^ϕ for a 3D nematic liquid crystal, with $\phi=0.44$. The data were taken from a 90^3 lattice and averaged over 20 initial conditions. The symbols correspond to times 40 (\square), 119 (\triangle), 260 (\diamond), 570 (\oplus), and 1200 ($*$) cell dynamics steps. The solid curve is the Bray-Puri function [7] for $n=2$. Inset: A plot of $\ln l(t)$ vs $\ln t$, with $l(t)$ defined by $C(l(t),t)=0.5$. The straight line is the least-squares fit, with a slope 0.44.

that for $kl(t) \gg 1$ the structure factor should be proportional to the total defect density. The latter scales as $l(t)^{-n}$ for the $(d-n)$ -dimensional defects occurring in n -dimensional vector fields. Demanding a factor $l(t)^{-n}$ from (7) requires the tail behavior $g(x) \sim x^{-(d+n)}$ for $x \rightarrow \infty$. This argument, focusing directly on the defects, generalizes to NLC's, so for $d=3$ we expect $\chi=5$ or 6 depending on whether strings or monopoles dominate.

For the $d=2$, $n=2$ system both $\pm \frac{1}{2}$ and ± 1 defects have pointlike vortex cores, so we would expect the same result $\chi=d+n=4$ for the two-dimensional (2D) NLC and the $O(2)$ system. A least-squares fit to the structure function tail (Fig. 2) gives the value $\chi=4.0 \pm 0.1$, in good agreement with this prediction. For amusement, we include in Fig. 1 the BP prediction [7] for the scaling function of the $O(2)$ system, with the abscissa scaled to give the best fit by eye. Note that $C(r)$ for the $O(2)$ system is simply $\langle \hat{\phi}(\mathbf{r}) \cdot \hat{\phi}(\mathbf{0}) \rangle$, different from the function $\langle d(\hat{\phi}(\mathbf{r}) \cdot \hat{\phi}(\mathbf{0}))^2 - 1 \rangle / (d-1)$ appropriate to the NLC. However, with the representation $\hat{\phi} = (\cos\theta, \sin\theta)$, the two functions are related through the transformation $\theta \rightarrow 2\theta$ of the angles, the same transformation that maps the $\pm \frac{1}{2}$ vortices of the NLC into the ± 1 vortices of the $O(2)$ model. Seen in this light, the comparison with the BP function is quite natural. In fact, it is possible to show that the dynamics of the $O(2)$ model and the $d=2$ nematic become isomorphic after this change of variable [20].

In the bulk NLC the situation is less clear. In the $d=3$, $O(3)$ model the only stable defect is the monopole. The spins in a string defect can be continuously moved towards

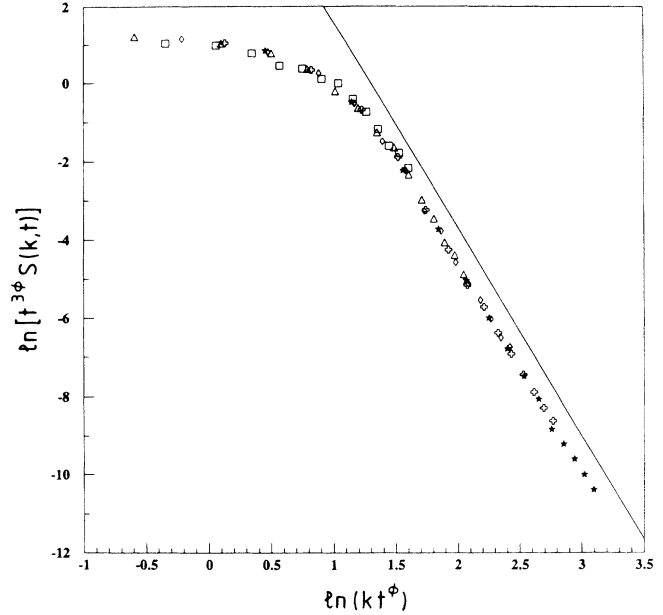


FIG. 4. Log-log scaling plot for the structure function of the 3D nematic liquid crystal, with $\phi=0.44$. Only k values up to $\frac{1}{2}$ of the zone boundary are included. The symbols have the same meanings as in Fig. 3. The straight line has slope -5.3 .

the direction parallel to the string axis without creating discontinuities (“escape in the third dimension”). Any strings present after the quench therefore quickly disappear. This process is not possible with a $\pm \frac{1}{2}$ string: Such a deformation would lead to a line of discontinuities in the plane perpendicular to the string axis. The presence of $\pm \frac{1}{2}$ strings would suggest the value $\chi=5$, analogous to an $O(2)$ system, rather than the naive $\chi=6$ which would be obtained by simply putting $n=3$ in the BP result.

Indeed we measure (Fig. 4) $\chi=5.3 \pm 0.1$, closer to the value of $\chi=5$ which would be expected if strings rather than monopoles were the dominant topological defect on the time scales considered. A value of χ between 5 and 6 suggests that both types of defect are playing a significant role. If there were a single characteristic length scale $l(t)$, however, the string contribution would dominate for $kl(t) \gg 1$, giving a k^{-5} tail. It is possible, therefore, that the predominance of strings is a transient effect, and that the string density decreases proportionately more rapidly than the monopole density. However, we find no evidence for any change in χ up to the latest times observed.

For completeness, we also include the BP function for $n=2$ in Fig. 3, with the abscissa again scaled to give the best fit by eye, although the justification for this comparison is not as clear as for $d=2$. The fit is again quite good. It should be noted, however, that the $n=3$ BP function does not fit perceptibly worse.

Wong *et al.* have measured $S(k)$ experimentally in caesium perfluoro-octanoate in both two and three dimensions [14]. For $d=2$, they find good agreement with both the BP prediction and our simulation data, measuring $\chi=4.1 \pm 0.3$. For $d=3$, however, they find $\chi=6.0 \pm 0.3$, in accord with the BP prediction for $n=3$ but clearly

different from our simulation result, which is closer to the BP result for $n=2$. The discrepancy may possibly be due to the inadequacy of the equal constant approximation to describe monopoles in real NLC's. Goldhaber [21] has shown that, in the equal constant approximation, the monopole can deform into a thin "flux tube" with all the flux out of a monopole concentrated in it. Such processes are not observed experimentally. Indeed it is found in [5] that with a small perturbation away from the equal constant approximation the monopoles become stable. In addition, they find that such monopoles have a cylindrical rather than a spherical symmetry, suggesting that the equal constant approximation may alter the properties of the monopoles and hence their role in the phase ordering.

We now discuss the results for the growth exponent ϕ . As we noted above, the data from the $d=2$ system do not fit the form $l(t) \sim t^\phi$ for any ϕ (inset, Fig. 1). This may again be a transient effect or could be caused by a gradual freezing of the system into a metastable configuration, as was observed to happen for $D=0.5$, $E=1.3$. It has been suggested [20] that such freezing could be caused by a weak pinning of the vortices to favorable locations at centers of plaquettes. Similar simulations of a 2D vector model [2], however, achieved an approximate power-law scaling, although the value of the exponent ϕ increased from around $\frac{2}{3}$ at early times to 0.50 later. We have run our simulations for a similar number of updates but find no evidence for this type of behavior. On the contrary, we find the effective value of ϕ decreases at later times. Similar behavior has been observed by Desai and Somoza [20].

For the $d=3$ system we found that the data scaled excellently with $l(t) \sim t^{0.44}$ over a wide range of times ($t=40$ to $t=1200$; the $t=40$ data, however, lie slightly outside the main scaling curve). From a log-log plot of $l(t)$ against t (inset, Fig. 3) we determine $\phi=0.44 \pm 0.01$. Mondello and Goldenfeld [3] and Toyoki [22] found $\phi=0.45 \pm 0.01$ for the $d=3$, $O(2)$ model using a cell-dynamics simulation. These results are at variance with a number of analytic treatments [7,8] suggesting $\phi = \frac{1}{2}$. However, we cannot be sure the system is in the asymptotic regime in our simulation and longer runs may eventually reach an exponent value of $\frac{1}{2}$.

To summarize, we have simulated a spin model corresponding to a nematic liquid crystal in the equal constant approximation. We observe the tail in the structure function to decay as $S(k) \sim k^{-4.0 \pm 0.1}$ in $d=2$ and as $S(k) \sim k^{-5.3 \pm 0.1}$ in $d=3$. For $d=3$ this differs from the result derived by BP for the $O(3)$ model and with the experimental result $\chi=6 \pm 0.3$ [14]. We believe this is due to the presence of nonintegrally charged topological defects ($\pm \frac{1}{2}$ strings) in the nematic which are absent from the $O(3)$ model and which dominate at the times scales of the simulation, giving results closer to the BP prediction for $n=2$. We find a growth exponent $\phi=0.44 \pm 0.1$ in $d=3$, consistent with earlier simulation results [3,22] for $O(2)$ models.

A. B. thanks R. C. Desai, S. Puri, A. M. Somoza, A. P. Y. Wong, and B. Yurke for discussions. R. B. acknowledges the SERC (United Kingdom) for financial support.

-
- [1] H. Toyoki and K. Honda, *Prog. Theor. Phys.* **78**, 237 (1987); H. Nishimori and T. Nukii, *J. Phys. Soc. Jpn.* **58**, 563 (1988); S. Puri and C. Roland, *Phys. Lett. A* **151**, 500 (1990); A. Coniglio and M. Zannetti, *Europhys. Lett.* **10**, 575 (1989); A. J. Bray, *Phys. Rev. B* **41**, 6724 (1990); T. J. Newman and A. J. Bray, *J. Phys. A* **23**, 4491 (1990); A. J. Bray and K. Humayun, *Phys. Rev. Lett.* **68**, 1559 (1992).
- [2] M. Mondello and N. Goldenfeld, *Phys. Rev. A* **42**, 5865 (1990).
- [3] M. Mondello and N. Goldenfeld, *Phys. Rev. A* **45**, 657 (1992).
- [4] I. L. Chuang, N. Turok, and B. Yurke, *Phys. Rev. Lett.* **66**, 2472 (1991).
- [5] I. L. Chuang, R. Durrer, N. Turok, and B. Yurke, *Science* **251**, 1336 (1991).
- [6] T. J. Newman, A. J. Bray, and M. A. Moore, *Phys. Rev. B* **42**, 4514 (1990); K. Humayun and A. J. Bray, *J. Phys. A* **23**, 5897 (1990).
- [7] A. J. Bray and S. Puri, *Phys. Rev. Lett.* **67**, 2670 (1991); see also H. Toyoki, *Phys. Rev. B* **45**, 1965 (1992).
- [8] A. J. Bray and K. Humayun, *J. Phys. A* **25**, 2191 (1992); Fong Liu and G. F. Mazenko, *Phys. Rev. B* **45**, 6989 (1992).
- [9] H. Toyoki, *Phys. Rev. A* **42**, 911 (1990).
- [10] G. Porod, in *Small-Angle X-Ray Scattering*, edited by O. Glatter and O. Kratsky (Academic, New York, 1982); P. Debye, H. R. Anderson, and H. Brumberger, *J. Appl. Phys.* **28**, 679 (1957); Y. Oono and S. Puri, *Mod. Phys. Lett. B* **2**, 861 (1988).
- [11] H. Toyoki, *J. Phys. Soc. Jpn.* **60**, 1153 (1991); **60**, 1433 (1991).
- [12] L. Michel, *Rev. Mod. Phys.* **52**, 617 (1980); M. Kléman, *Points, Lines, and Walls, in Liquid Crystals, Magnetic Systems, and Various Ordered Media* (Wiley, New York, 1983).
- [13] A. Pargellis, N. Turok, and B. Yurke, *Phys. Rev. Lett.* **67**, 1570 (1991).
- [14] A. P. Y. Wong, P. Wiltzius, and B. Yurke, *Phys. Rev. Lett.* **68**, 3583 (1992); A. P. Y. Wong, P. Wiltzius, R. G. Larsen, and B. Yurke (unpublished).
- [15] P. G. de Gennes, *The Physics of Liquid Crystals* (Clarendon, Oxford, 1974).
- [16] Y. Oono and S. Puri, *Phys. Rev. A* **38**, 434 (1988).
- [17] Y. Oono and S. Puri (Ref. [10]).
- [18] Other definitions of $l(t)$ lead to very similar results.
- [19] A. J. Bray, *Phys. Rev. E* (to be published).
- [20] R. C. Desai and A. M. Somoza (private communication).
- [21] A. S. Goldhaber, *Phys. Rev. Lett.* **63**, 2158 (1989).
- [22] H. Toyoki, *J. Phys. Soc. Jpn.* **60**, 1433 (1991).